

Phase Separation in Two-Dimensional Fluid Mixtures

Gregory Leptoukh, Bowe Strickland, and Christopher Roland

Department of Physics, North Carolina State University, Raleigh, North Carolina 27695

(Received 28 November 1994)

The phase separation of two-dimensional fluid mixtures was investigated with molecular dynamics simulations. The behavior of both single-component and binary mixtures as a function of temperature, volume fraction, and average fluid density was considered. In both systems, the diffusive coalescence of clusters is the primary mechanism of growth. In binary systems, the shape transformations of merging droplets induce important long-range flow in the system.

PACS numbers: 64.60.Qb, 05.70.Ln, 61.20.Ja, 64.75.+g

When a fluid is rapidly quenched from the disordered, high-temperature, single-phase region of its phase diagram to a point inside of the coexistence curve, it orders kinetically [1]. A long-wavelength instability creates a morphology of interpenetrating domains, which grow to macroscopic size as time goes on. At late times, this growth often involves a single, time-dependent length scale, the average domain size $R(t)$, to which all spatial quantities scale. For example, the time-dependent structure factor $S(k, t)$, with wave number k , displays the scaling behavior $S(k, t) = R(t)^d F(x)$, where $x = kR(t)$, d is the dimensionality of the system, and $F(x)$ is the time-independent shape function. Furthermore, the growth of the average domain size often follows a power law $R(t) \sim t^n$, with growth exponent n . This exponent is the focus of much investigation, as it intimately reflects the mechanisms which drive the phase separation process. It is generally believed that the growth exponent together with the time-independent shape functions characterize a given universality class. For example, in binary-alloy systems growth is determined solely by the thermodynamic forces driving the phase separation, so that the exponents are independent of dimensionality of the system. They do, however, depend crucially upon the presence of conservation laws for the order parameter. For a nonconserved system (model A [2]), growth is curvature driven with an exponent of $\frac{1}{2}$ [3]. If the system involves a conserved order parameter (model B), ordering takes place through the diffusive transport of material through the bulk, i.e., the classical Lifshitz-Slyozov mechanism, with an asymptotic exponent of $\frac{1}{3}$ [4].

In fluid systems, this situation is more complicated due to competing and transient growth mechanisms brought about by the hydrodynamic modes of the system. The latter allows for the transport of the ordered domains, so that droplet coalescence is important [5]. The predicted scenario for 3D binary fluid mixtures is the following: For low volume fractions, growth takes place via the diffusive coalescence of droplets followed by a crossover to Lifshitz-Slyozov growth. Both of these mechanisms give a $R \sim t^{1/3}$ growth law, albeit with differing amplitudes. As the volume fraction is increased, hydrodynamic flow driven by surface tension effects becomes more and

more important. Siggia then predicts a crossover to $R \sim t$ growth, valid for a symmetric quench [6]. Experiments on fluids [7,8], as well as numerical simulations [9], have verified aspects of this picture.

In contrast, the nature of the phase separation of 2D fluid systems has remained controversial. For symmetric quenches, Furukawa [10,11] has predicted a late-time accelerated $n = \frac{2}{3}$ growth based on inertial effects, while a competing theory based on linear hydrodynamics predicts $n = \frac{1}{2}$ [12]. Numerical studies have also yielded conflicting evidence: Langevin simulations of model H [13] and lattice-gas simulations [14] are consistent with an $n = \frac{2}{3}$ exponent, while molecular dynamics (MD) simulations at different densities have yielded both values [15,16].

To address the nature of phase separation in 2D fluid systems [17], we have carried out extensive MD studies of both single-component and binary fluid mixtures, which involves the coupling between a conserved order parameter (relative fluid density) and the velocity fields of the fluid. Simulations as a function of temperature, volume fraction, and fluid density were carried out. We find that for single-component fluids and off-symmetric binary fluid mixtures, quenched into the unstable region of the phase diagram, the coalescence of droplets is the most important growth mechanism, with exponents $n \leq \frac{1}{2}$. For symmetric quenches of binary fluids, growth is consistent with $n = \frac{1}{2}$ based on the diffusion and merging of interfaces as predicted by linear hydrodynamics. We find no evidence of any significant Lifshitz-Slyozov growth over the time scales of our simulations.

We now give details of our simulations. Atoms of the single-component fluid were modeled with the cut and shifted (12-6) Lennard-Jones potential (cut off at 2.5σ), for which the phase diagram is well known [18,19]. The binary fluid mixture consisted of two species, labeled A and B . The interaction potential was taken to be an extended (12-3) Lennard-Jones potential of the form

$$U(r_{ij}) = 4\epsilon \left[\left(\frac{\sigma}{r_{ij}} \right)^{12} - (2\delta_{i,j} - 1) \left(\frac{\sigma}{r_{ij}} \right)^3 \right],$$

where $r_{ij} = r_i - r_j$ is the distance (truncated at 4.2σ), between the species i and j . Forces between "like" species

are therefore attractive and repulsive between “unlike” species. The specific form of these potentials was chosen so as to make contact with previous simulations [15–19]. Square systems with periodic boundary conditions were used. Simulations were carried out for $\sim 17\,000$ atoms over density ranges of $\rho\sigma^2 = 0.2$ to 0.8 , using the standard Verlet algorithm [20]. Velocity rescaling was used to keep the systems at a constant temperature, although some constant energy simulations were carried out [18]. Generally, an integration time step of 0.02τ (single-component system) and 0.005τ (binary mixture) was found to be adequate, where the time scale is $\tau = (m\sigma^2/\epsilon)^{1/2}$. The time step was, however, further reduced at high temperatures. Unless otherwise indicated, all the data presented were averaged over at least ten independent runs. Initial configurations were prepared by scaling atoms on a hexagonal lattice to their proper density, and then, in the case of a binary mixture, labeling them *A* or *B* at random, in their proper proportion. Volume fractions ϕ between 0.1 to 0.5 (symmetric quench) were simulated. During the simulations, a number of quantities were monitored. Chief of these was the circularly averaged structure factor $S(k, t)$, from which two measures of length were obtained: $R_1(t) = 2\pi/k_1(t)$, where $k_1(t)$ denotes the first moment of the structure factor; and $R_c(t)$, which denotes the first zero of the pair-correlation function $g(r, t)$.

We first present the results for the single-component fluid. Figure 1 shows sample configurations for a critical quench ($\rho\sigma^2 = 0.325$) at different temperatures. After the quench, the system forms small, *finite-sized*, irregularly shaped domains. Growth takes place primarily through the coalescence of these domains: Monomers, which move ballistically and strike the domains, set the clusters into linear and rotational motion. These then perform inelastic collisions with other clusters which then coalesce. At the same time, the surface tension acts to reshape the cluster into a circular shape, thereby reducing the surface free energy. At low temperatures, this process is almost completely inhibited so that a variety of “lattice animals” form. High temperatures are almost completely dominated by critical fluctuations.

The effective growth exponents for the single-component system over the entire temperature range is shown in Fig. 2. This curve was obtained by fitting R_1 by a power law form over $\sim 500\tau$. Other measures of length show similar behavior. The growth exponents display a maximum value of $n = 0.55 \pm 0.06$ near $T \approx 0.72T_c$, consistent with a coalescence mechanism of clusters [21]. Indeed, an examination of the simulations shows that the rate of diffusion is maximized at this temperature. At lower temperatures, the rate of cluster diffusion is reduced, giving lower exponents over the time scale of the simulation. At the lowest temperatures, the clusters are almost completely frozen.

At temperatures greater than $T \sim 0.72T_c$, critical fluctuations play an important role: monomers proliferate, the interfacial roughness becomes large, and the definition of the

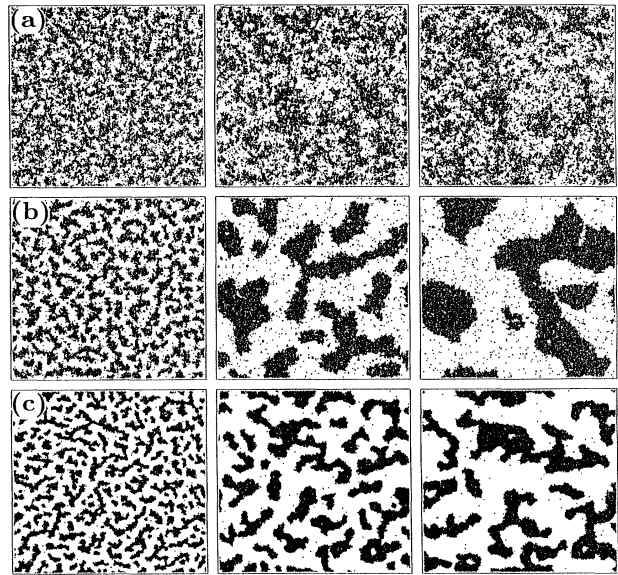


FIG. 1. Sample configurations showing phase separation in a single-component fluid as a function of temperature: (a) $T/T_c = 0.89$, (b) $T/T_c = 0.71$, and (c) $T/T_c = 0.54$, at times 20τ , 200τ , and 400τ , left to right panels, respectively.

cluster becomes ambiguous. In this regime, length scales should be measured in terms of the correlation length $\xi = (1 - T/T_c)^{-\nu}$ and times in terms of the correlation time $\tau_\xi = \xi^z$, where ν and z are critical exponents. Indeed, good data collapse is achieved for $T \geq 0.75T_c$ with $\nu = 1$, $\eta = 0.25$, and $z = 4 - \eta$ consistent with the dynamical scaling hypothesis (see inset of Fig. 2) [22]. Thus, our simulations in the critical region are essentially at “early times” with regard to the phase separation processes

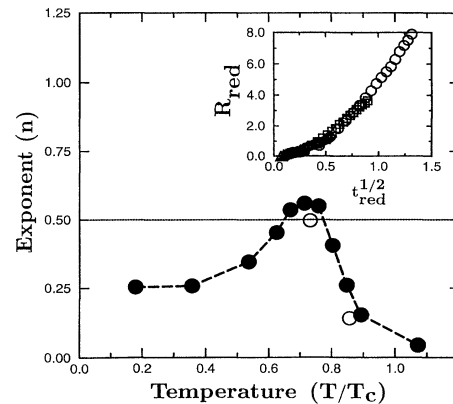


FIG. 2. Effective growth exponents n as a function of temperature for single-component system. The open symbols are exponents derived from *constant energy* runs (four runs). The inset shows the scaling of $R_{\text{red}} = [R_1(t) - R_1(t=0)]/\xi$ vs $t_{\text{red}}^{1/2} = (t/\tau_\xi)^{1/2}$ in the critical region: circles, $T = 0.76T_c$; squares, $T = 0.80T_c$; diamonds, $T = 0.85T_c$; and triangles, $T = 0.89T_c$. Data are obtained from at least ten runs, except at $T = 0.18T_c$, $0.35T_c$, $0.84T_c$, and $0.89T_c$, which are from at least four runs.

[19]. This also explains the differences between constant temperature and constant energy runs observed in previous simulations [18]. In the constant energy simulations, the actual temperature of the system rises because potential energy is converted into kinetic energy as the phase separation proceeds. Thus, for constant energy simulations with initial $T \geq 0.54T_c$, the actual temperature of the system is such that the system is in the critical regime, and the growth exponent decreases. To test this, we have carried out a number of constant energy simulations for initial $T = 0.54T_c$ and $0.80T_c$. These runs, however, have actual late-time temperatures of $0.73T_c$ and $0.86T_c$, respectively [23]. The growth exponents at these actual temperatures are close to those of the constant temperature runs.

We now turn to phase separation in binary fluid mixtures, at high fluid densities. Figure 3 shows sample configurations ($\rho\sigma^2 = 0.74$) for different volume fractions. After a symmetric quench, the instability forms a complicated and now *interconnected* network of ordered domains, which then coarsens via the diffusion of interfaces. In the case of off-symmetric quenches, isolated droplets form and grow via droplet coalescence. As in the case of the single-component fluid, there is no evidence of any Lifshitz-Slyozov growth.

Figure 4 summarizes the measured growth exponents for the binary fluid mixture, as a function of both temperature and volume fraction. In this case the exponents were obtained by power law fits to R_c , although other measures of length gave completely similar results. In general, the behavior of the growth exponents with temperature shows trends similar to that of the single-component fluid. For

off-symmetric quenches, the maximum growth exponent is achieved at intermediate reduced temperatures $k_B T/\epsilon \approx 12$ to 16. At lower temperatures, the growth law is always reduced, reflecting the decrease in the rate of droplet diffusion. For off-symmetric quenches at low temperatures, the system is virtually frozen over the time scales of the simulations. The growth exponent is largest for the symmetric quench. For temperatures less than 20, $n = 0.46 \pm 0.05$ consistent with the $t^{1/2}$ law based on linear hydrodynamics. At high temperatures, the growth exponent decreases because of the high thermal fluctuations. Simulations at all other fluid densities gave exponents $n \leq 0.5$, consistent with the coalescence mechanisms.

While diffusive coalescence is the main mechanism of growth in both of the fluid systems, the source of the fluctuations leading to the movement of droplets differs. In binary fluid mixtures, surface tension effects resulting from the reshaping of droplets play a crucial role. Consider a binary collision between two droplets. Just after touching, the combined droplet has, roughly speaking, a nonsymmetric, ellipsoidal shape. Surface tension then induces rapid shape relaxations, which transform the droplet into a circular shape. This induces considerable flow in the surrounding fluid medium, and, depending upon the specific geometry of the system, induces multiple collision events (see Fig. 5). This has recently been observed in experimental fluid systems [24]. The effect that the induced fluid flow has on the system depends very much on the droplet size. For the low volume fractions, when the size of the droplet is small compared to the distances separating them, the effect of the induced flow is small. It does, however, increase noticeably for $\phi \geq 0.30$, when such events dominate. In the case of a symmetric quench, when the domain structure is percolating, the induced flow may dominate and spread over a large fraction of the system. Naturally, the shape transformations taking place after the merging of droplets do not play such a role in single-component

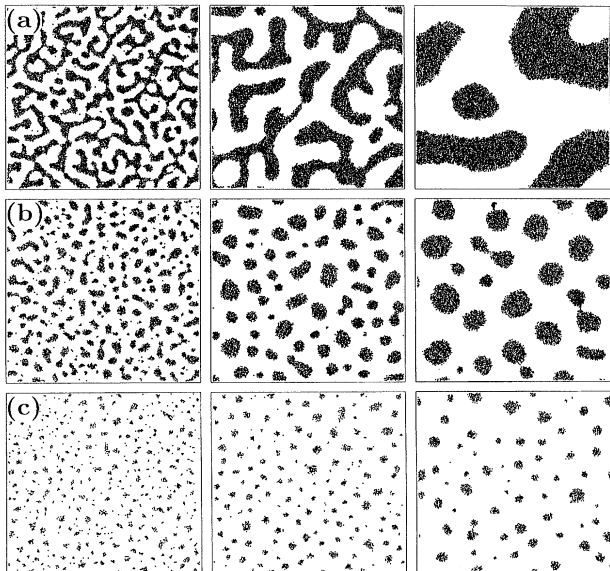


FIG. 3. Sample configurations showing phase separation in binary fluid system for different volume fractions: (a) $\phi = 0.5$ (symmetric quench), (b) $\phi = 0.3$, and (c) $\phi = 0.1$ at times 5τ , 12.5τ , and 52.5τ . Only the minority species is shown. Other parameters are $\rho\sigma^2 = 0.74$ and $k_B T/\epsilon = 2$.

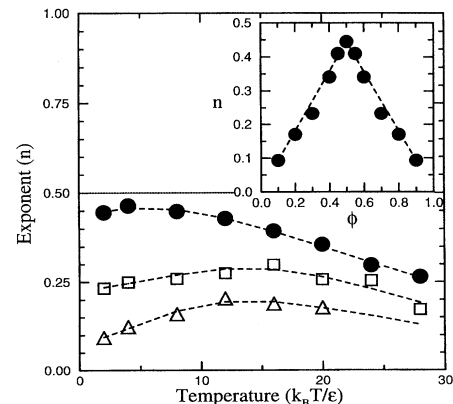


FIG. 4. Effective growth exponents n as a function of the reduced temperature $k_B T/\epsilon$ for symmetric $\phi = 0.5$ (solid circles, 14 runs for $T \leq 20$), $\phi = 0.30$ (open squares, four runs), and $\phi = 0.1$ (open triangles, four runs). The inset shows n vs ϕ for a reduced $T = 2$ (ten runs).

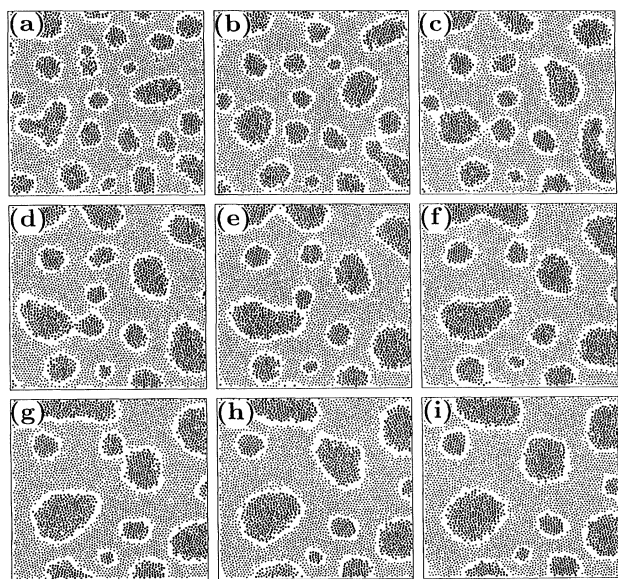


FIG. 5. Partial configurations showing multiple coalescence events for $\phi = 0.30$ and a reduced $T = 2$. The sequence (a) to (i) shows configurations beginning at 12.5τ , each a time period 2.5τ apart.

systems. This is because there is no medium present so that flows cannot be communicated readily throughout the system. Monomer and small droplet collisions, as well as thermal fluctuations, are the main causes of droplet movement in single-component systems.

In summary, we have carried out extensive MD simulations of phase separation of both single-component and binary fluid mixtures, as a function of temperature, volume fraction, and fluid densities. The diffusion and subsequent coalescence of droplets is the main mechanism of growth, which give growth exponent $n \leq \frac{1}{2}$ [25]. Over the time regime of our simulations, there is no evidence of an accelerated $n = \frac{2}{3}$ growth. In binary fluid mixtures, the reshaping of droplets during a collision event plays a significant role in inducing long-range droplet flow.

We would like to thank Dr. M. Laradji for useful discussions and the North Carolina Supercomputing Center for significant amounts of computer time. Acknowledgment is made to the donors of the Petroleum Research Fund administered by the American Chemical Society for support of this work, under Grant No. 27092-G9.

- [1] See, for example, J.D. Gunton, M. San Miguel, and P. Sahni, in *Phase Transitions and Critical Phenomena*, edited by C. Domb and J.L. Lebowitz (Academic Press, New York, 1983), Vol. 8.
- [2] P. C. Hohenberg and B.I. Halperin, *Rev. Mod. Phys.* **47**, 435 (1977).
- [3] S. M. Allen and J. W. Cahn, *Acta Metall.* **27**, 1085 (1979); K. Kawasaki, M. C. Yalabik, and J. D. Gunton, *Phys. Rev. A* **17**, 455 (1978).

- [4] I. M. Lifshitz and V. V. Slyozov, *J. Phys. Chem. Solids* **19**, 35 (1961).
- [5] K. Binder and D. Stauffer, *Adv. Phys.* **25**, 343 (1976).
- [6] E. D. Siggia, *Phys. Rev. A* **20**, 595 (1979).
- [7] N. Wong and C. Knobler, *J. Chem. Phys.* **69**, 725 (1978); *Phys. Rev. A* **24**, 3205 (1981); Y. C. Choi and W. Goldberg, *ibid.* **20**, 2105 (1979); E. Siebert and C. Knobler, *Phys. Rev. Lett.* **54**, 819 (1985).
- [8] F. Perot, P. Guenoun, T. Baumberger, D. Beysens, Y. Garrabos, and B. Le Neindre, *Phys. Rev. Lett.* **73**, 688 (1994).
- [9] T. Koga and K. Kawasaki, *Phys. Rev. A* **44**, 817 (1991); S. Puri and B. Duenweg, *ibid.* **45**, 6977 (1992); O. T. Valls and J. E. Farrell, *Phys. Rev. E* **47**, 36 (1993).
- [10] H. Furukawa, *Phys. Rev. A* **30**, 1052 (1984); **31**, 1103 (1985).
- [11] H. Furukawa, *Adv. Phys.* **34**, 703 (1985).
- [12] M. San Miguel, M. Grant, and J. D. Gunton, *Phys. Rev. A* **31**, 1001 (1985).
- [13] O. T. Valls and G. F. Mazenko, *Phys. Rev. B* **38**, 11 643 (1985); J. E. Farrell and O. T. Valls, *ibid.* **40**, 7027 (1989); **42**, 2353 (1990).
- [14] F. I. Alexander, S. Chen, and D. W. Grunau, *Phys. Rev. B* **48**, 634 (1993).
- [15] W. J. Ma, A. Maritan, J. Banavar, and J. Koplik, *Phys. Rev. A* **45**, 5347 (1992).
- [16] E. Valasco and S. Toxvaerd, *Phys. Rev. Lett.* **71**, 388 (1993); P. Ossadnik, M. F. Gyure, H. E. Stanley, and S. Glotzer, *ibid.* **72**, 2498 (1994).
- [17] For a discussion of the early stages, see S. W. Koch, R. C. Desai, and F. F. Abraham, *Phys. Rev. A* **26**, 1015 (1982).
- [18] F. F. Abraham, S. W. Koch, and R. C. Desai, *Phys. Rev. Lett.* **49**, 923 (1982); S. W. Koch, R. C. Desai, and F. F. Abraham, *Phys. Rev. A* **27**, 2152 (1983).
- [19] R. Yamamoto and K. Nakarish, *Phys. Rev. B* **49**, 14958 (1994).
- [20] See, for example, *Computer Simulations Using Particles*, edited by P. W. Hockney and J. W. Eastwood (McGraw Hill, New York, 1981).
- [21] The slightly higher value of the exponent derived from R_1 is due to difficulties in sampling the peak region for the finite-sized system. Other measures of length give lower exponents. For example, R_c , the best measure of length, gives a maximum value of $n = 0.52 \pm 0.05$. However, because it is difficult to unambiguously probe the domain structure in the critical regime with $g(r, t)$, we chose to present results derived from $S(k, t)$.
- [22] See, for example, H. E. Stanley, *Introduction to Phase Transitions and Critical Phenomena* (Oxford Press, New York, 1971).
- [23] Such increases in temperature are expected, even for deep quenches, because the system evolves from similar initial states with a large interface density to the same final ordered state, so that roughly similar amounts of potential energy are converted into kinetic energy, albeit at different rates.
- [24] H. Tanaka, *Phys. Rev. Lett.* **72**, 1702 (1994).
- [25] In addition to the physical reasons stated, it is also likely that there are logarithmic corrections to the exponents in 2D.